IEEE Access
Multidisciplinary | Rapid Review | Open Access Journal

SPECIAL SECTION ON KEY ENABLING TECHNOLOGIES FOR PROSUMER ENERGY MANAGEMENT

Received July 13, 2020, accepted July 23, 2020, date of publication September 1, 2020, date of current version September 11, 2020.

Digital Object Identifier 10.1109/ACCESS.2020.3018587

Optimal Operation of Integrated Energy System Based on Exergy Analysis and Adaptive Genetic Algorithm

HAOYONG CHEN[1], (Senior Member, IEEE), SIMIN CHEN[1], (Student Member, IEEE), MING LI[2], AND JINBIN CHEN[1]

[1]School of Electric Power Engineering, South China University of Technology, Guangzhou 510640, China
[2]Guangdong Planning and Designing Institute of Telecommunications Company Ltd., Guangzhou 510630, China

Corresponding author: Haoyong Chen (eehychen@scut.edu.cn)

This work was supported in part by the National Natural Science Foundation of China under Grant 51937005, and in part by the National Key Research and Development Program of China under Grant 2016YFB0900100.

ABSTRACT Due to the rising tensions surrounding the energy industry in response to the depletion of non-renewable energy sources and pollution of the environment, it is especially important to improve the energy utilization rate of integrated energy systems (IESs). Exergy is an important index to measure energy quality. Therefore, this paper proposes an IES operation optimization method based on exergy analysis and an adaptive genetic algorithm. First, based on the energy network theory, a unified expression of the exergy transfer process is given, and the energy level factor is introduced to evaluate the energy quality. Second, the steady-state expression of different forms of exergy in the energy transfer line is given. Third, the exergy economic model of the IES is established by combining exergy analysis, and the solution process of the adaptive genetic algorithm is given. Finally, the operation optimization simulation and analysis of an IES in Bali are carried out to verify the effectiveness of the exergy analysis method and feasibility of the simulation method.

INDEX TERMS Exergy analysis, energy networks, exergy economic loss, energy utilization rate, self-adaptive genetic algorithm, integrated energy system.

NOMENCLATURE

A. INDEX

i	Type of energy ii = e (electricity), h (heat), p (pressure)
m	Starting section of energy transfer line
n	End section of energy transfer line

B. CONSTANTS

L	Inductive element
C	Capacitive element
R	Resistive element
χ_{i0}	Static value of intensive quantity
ε_i	Energy level coefficient
A	Sectional area of line
L	Line length
ρ_i	Density of energy transfer medium
c	Specific heat capacity of heat transfer medium
λ	Energy transfer coefficient
D	Diameter of energy transfer pipeline
c_{xe}	Electrical exergy price
η_{p}	Efficiency of circulating water pump
c_{xh}	Heat exergy price
S_{el}	Number of power network lines
S_{hl}	Number of thermal network lines
c_{e}	Electrical energy price
c_{h}	Heat energy price
$P_{\mathrm{e}}^{G_{min}} / \leq P_e^{G_{max}}$	Lower/upper active power output of power generator
$Q_e^{\mathrm{G}_{min}} / Q_e^{\mathrm{G}_{max}}$	Lower/upper reactive power output of power generator
$\chi_{emin} / \chi_{\mathrm{e\,max}}$	Lower/upper magnitude of nodes
$\theta_{\mathrm{e\,min}} / \theta_{\mathrm{e\,max}}$	Lower/upper phase angle of nodes
$\varphi_{\mathrm{e}}^{I_{\max}}$	Upper electric current of pipeline
$Tap_{i\,\mathrm{min}} / Tap_{i\,\mathrm{max}}$	Lower/upper transformer ratios

The associate editor coordinating the review of this manuscript and approving it for publication was Bin Zhou.

S_{Tap}	Transformer ratio set
$P_{\mathrm{h}}^{\mathrm{G\,min}}/P_{\mathrm{h}}^{\mathrm{G\,max}}$	Lower/upper thermal outputs of gas-fired boilers
$\chi_{\mathrm{h\,min}}/\chi_{\mathrm{h\,max}}$	Lower/upper water temperature of each node
$P_{\mathrm{h}}^{l\,\mathrm{min}}/P_{\mathrm{h}}^{l\,\mathrm{max}}$	Lower/upper heat power of thermal lines
$\varphi_{\mathrm{p\,min}}/\varphi_{\mathrm{p\,max}}$	Lower/upper volume flow of thermal lines

C. VARIABLES

Φ_i	Generalized displacement (e.g., charge Φ_{e}, entropy Φ_{h}, volume Φ_{p})
φ_i	Generalized extensive flow (e.g., electric current φ_{e}, entropy flow φ_{h}, volume flow φ_{p})
χ_i	Generalized intensive quantity (e.g., electric potential χ_{e}, temperature χ_{h}, pressure χ_{p})
X_i	Generalized momentum (e.g., flux X_{e}, temperatureX_{h}, pressure X_{p})
E_i	Energy (e.g., electrical energy E_{e}, heat energy E_{h}, pressure energy E_{p})
E_{xi}	Exergy (e.g., electrical exergy E_{xe}, heat exergy E_{xh}, pressure exergy E_{xp})
J_i	Generalized displacement flow density
J_{Exi}	Exergy flow density
σ_i	Generalized displacement source strength
x_g	The function of generalized displacement source strength with line length
ΔP_x	Change of exergy power (e.g., ΔP_{xe}, ΔP_{xh}, ΔP_{xp})
ΔP	Change of energy power (e.g.,ΔP_{e}, ΔP_{h}, ΔP_{p})
J_E	Electrical exergy price
k_{p}	Transfer coefficient of generalized displacement volume
f	Friction coefficient of fluid flow
C_{loss}	Total loss of energy network exergy economy
P_{e}^{l}	Active power of electrical line
Q_{e}^{l}	Reactive power of electrical line
$\chi_{\mathrm{h}}^{'}$	Difference between node temperature and ambient temperature of thermal network $\chi_{\mathrm{h}}^{'} = \chi_{\mathrm{h}} - \chi_0$

I. INTRODUCTION

A. BACKGROUND

Due to increasing concerns regarding the environmental pollutants produced by coal-fired power generators and the low-efficiency energy utilization of conventional electrical power grids, which focus on electrical energy utilization but ignore other kinds of energy utilization (e.g., heating energy) [1], many researchers are searching for more environmentally friendly and less costly ways to supply energy. The integrated energy system (IES), which integrates cogeneration units, heat pumps, and LiBr absorption refrigerators [2], [3], is considered a promising way to optimize the structure of energy utilization. The core part of the IES is a set of cogeneration units, which supply electricity to residents while simultaneously meeting heat demands with recovered waste heat produced in the power generation process. The energy efficiency of an IES can reach over 80% by integrating various forms of power generation into the same regional network [4]. Thus, IESs can realize complementary utilization of different types of energy and greatly improve the efficiency and flexibility of the system through cascade utilization of different types of energy.

Research on IESs can be categorized into four topics: component modelling, IES planning, IES operation optimization and IES control [5]. Precisely setting up a model of components for an IES provides the foundation for the other three research topics. The goal of IES planning is to determine the optimal capacity sizing and location of generation units to satisfy the long-term requirement of thermal and electricity loads subject to the constraint of the investment budget [6]. After IES planning, IES operation optimization aims to optimize the outputs of electric and thermal power to obtain the solution with the best combination of high energy efficiency, low operational cost, and low emissions [7]. Finally, the IES control strategy ensures the IES operates safely and steadily in real-time conditions [8]. It is worth pointing out that the strategies of both long-term planning and short-term control are associated with the operational optimization stage either directly or indirectly. Thus, appropriately determining the optimal operational solution is one of the key problems in IESs.

B. LITERATURE REVIEW

Considerable research has been conducted on the operation optimization of IESs [9]. Nikmehr and Najafi-Ravadanegh [10] set up the optimal economic operational model of IESs to minimize the total cost of generation and greenhouse gas emissions. However, thermal supply and demand are not taken into consideration in the model. Wang *et al.* [11] proposed a joint-operation model by flexibly scheduling various energy units to satisfy electric and thermal load demands. Xu *et al.* [12] further modelled the interaction power among multiple IESs and established the optimal energy management model for small-scale IESs. Similarly, for small-scale IESs, Tahir *et al.* [13] evaluated the potential operation risk with the conditional value at risk theory and formulated a stochastic risk-constrained economic dispatch model. In contrast, Jadidbonab *et al.* [14] viewed the whole of China as a typical large-scale IES and employed the EnergyPLAN simulation tool to optimize the combination of electricity and heating sources in the China IES. However, the above studies all made the strong assumption that the losses of cooling/heating energy and electricity energy during transmission could be neglected to facilitate the solution of the models. Ge *et al.* [15] appropriately assessed these energy losses in the transmission process and integrated them into the objective function of the coordinated operation model. Due to the nonconvex nonlinear terms of energy losses, a genetic algorithm (GA) with the penalty function method was employed to solve the proposed model.

Nevertheless, most existing studies [9]–[19] related to the optimal operation of IESs simply establish the objective function based on the first law of thermodynamics [20], which indicates that the total value of energy remains unchanged during the energy conversion process, without considering the attributes of energy quality and direction. Thus, the obtained strategies generally fail to accurately reflect the difference of energy quality. Note that the second law of thermodynamics [21] holds that the transfer of energy is directional and irreversible. According to the principle of energy degradation, when a system is spontaneous, the direction of the reaction must change along the direction of the total energy quality reduction of the system. For example, electrical energy can be entirely converted into thermal energy through the effect of resistance, whereas the same quantity of thermal energy fails to be converted into electrical energy with 100% efficiency regardless of the conversion method used. It can be intuitively concluded that electrical energy is of higher quality than thermal energy. To quantify the quality of different types of energy, exergy is defined as the largest theoretical energy potential that can be employed to do useful work [22], [23]. Based on this definition, the exergy efficiency of a practical residential IES was calculated by Ebrahimi *et al.* [24]. Wang *et al.* [25] assessed the exergy performance in three kinds of prime movers in IES (e.g., gas turbine, gas engine and diesel engine). Abbasi *et al.* [26] compared energy loss with exergy loss in a solar thermal integrated IES and illustrated that while the quantity of energy loss rose, the quantity of exergy loss decreased. Furthermore, a sensitivity analysis of energy and exergy performance was conducted to find the effect of key parameters on the IES by Mohammadi and Mehrpooya [27]. Although some works have investigated the exergy in IESs, obtaining the optimal IES operation strategy while considering exergy has not been fully studied. Furthermore, since the expression of exergy may be rather complex, incorporating exergy into an IES operation model can greatly increase the computational load of solving the model. Effectively solving the complex model is still an exasperating problem.

C. CONTRIBUTIONS

To address the above problem, a novel operation IES model considering exergy is proposed, and an adaptive GA is employed to effectively solve the proposed complex model. Considering the above background and literature review, the main contributions of this paper are summarized as follows:

1) The exergy index is defined to evaluate the quality of different types of energy in the IES.
2) To the best of the authors' knowledge, this is the first study to propose a novel operational IES model based on the *exergy* losses in the transmission process to produce an optimal operational solution with higher efficiency and quality of energy utilization. In contrast, most previous models [9]–[19] use *energy* losses as the optimization objectives.
3) An adaptive GA is employed to effectively solve the proposed nonlinear nonconvex optimization model.

The remainder of this study is organized as follows: Section II introduces the theory of energy networks in IESs, including the unified description of variables, the generalized description of energy and exergy, the generalized transfer equation of exergy and the solution equation of the energy network. In Section III, the transfer equations of specific forms of exergy in different energy transfer lines are given, including electrical exergy, heat exergy, and pressure exergy. In Section IV, the exergy economic model of the IES is established, and the objective function of exergy economic loss, network constraint, energy coupling element model, and the GA solution method under adaptive elitist retention strategy are given. The performance and effectiveness of the proposed method are evaluated in Section V based on numerical results obtained for an IES in Barry Island. The conclusions and contributions are presented in Section VI.

II. PROPOSED ENERGY NETWORK

In an IES, different energy subnetworks (e.g., electric power networks, heat networks, and gas networks) provide different energies to users, so these networks can be collectively referred to as an ''energy network''. The relationships between an energy network and its subnetworks can be compared with the transmission of information over the Internet and a local area network. For example, users do not know where the information is sent when using the network, and energy-coupling elements (e.g., generators, pumps, and heat exchangers) in the IES are equivalent to routers. Based on this physical level, the following basic theory of energy network is developed.

A. STATE VARIABLE DESCRIPTION OF ENERGY NETWORK

According to whether it is related to the quantity of matter, the parameters describing the state of the system can be divided into extensive and intensive properties. Among them, an extensive quantity is closely related to the quantity of a substance and has an additive property, whereas an intensive quantity is not closely related to the quantity of a substance. For example, in a thermal network, entropy is an extensive quantity, and temperature is an intensive quantity; in a hydraulic network, volume flow is an extensive quantity, and pressure is an intensive quantity; and in an electric network, charge is an extensive quantity, and electric potential is an intensive quantity. Therefore, according to the constitutive relationships between variables in different networks, constitutive relationships among variables of different energy subnetworks are shown in Fig. 1.

As shown in Fig. 1, according to the constitutive relationships among the variables of different energy subnetworks, four variables can be identified: generalized displacement, generalized extensive flow, generalized momentum, and generalized intensive quantity. Generalized displacement is equal to the product of the generalized intensive quantity and capacitive element; generalized extensive flow is equal

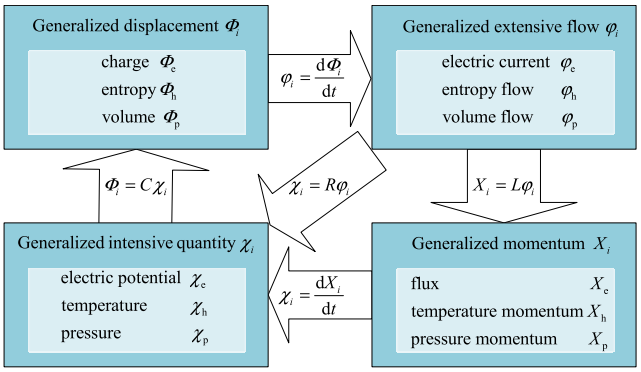

FIGURE 1. **Constitutive relationships among variables of different energy subnetworks.**

to the derivative of generalized displacement with respect to time; generalized momentum is equal to the product of the generalized extensive flow and inductive element; and generalized intensive quantity is equal to the derivative of generalized momentum with respect to time, and the product of the generalized extensive flow and resistive element.

B. GENERALIZED TRANSFER MODEL OF ENERGY AND EXERGY

The differential of any form of energy potential function is equal to the product of the differential of the corresponding basic intensive quantity and the conjugate basic extensive quantity, that is, any form of energy can be expressed by the same mathematical expression, which provides a mathematical basis for the unified study of the transfer and conversion process of different forms of energy in theory. Therefore, the differential equation of energy is shown in (1).

$$dE_i = \chi_i d\Phi_i. \tag{1}$$

However, in the process of energy utilization, we should not only pay attention to the change of energy ''quantity'' but also to the change of energy ''quality''. Exergy refers to the part of energy that can do useful work, reflecting the quality of energy. According to the first law of thermodynamics, energy is conserved, and the value of energy is greater than or equal to exergy. According to the second law of thermodynamics, it is found that energy transfer has obvious directionality. For example, electric energy can be completely converted into heat energy, but heat energy cannot be completely converted into electric energy. It can be seen that exergy will inevitably and irreversibly degenerate into unavailable energy in the process of energy transfer and conversion, and this energy loss to the environment is called exergy loss. The exergy of the system comes from the strength difference between the system and the environment. Thus, the generalized differential formula of any form of exergy is obtained as shown in (2).

$$dE_{xi} = (\chi_i - \chi_{i0}) d\Phi_i. \tag{2}$$

The energy level factor is introduced to evaluate the quality of energy according to static thermodynamics. The energy level factor corresponding to the *i*th form of energy in the system is equal to the ratio of the corresponding exergy differential to the energy differential, as shown in (3).

$$\varepsilon_i = \frac{dE_{xi}}{dE_i} = 1 - \frac{\chi_{i0}}{\chi_i}. \tag{3}$$

The analysis shows that the higher the energy level, the greater the value of energy utilization. For example, in an electric power network, the static state value of electric intensity quantity is zero, so the electric energy level is one, and the electric energy is equal to the electric exergy. In a thermal power network, the temperature static state value is not equal to zero, and the lower the temperature in the network, the smaller the energy level, the lower the thermal energy content and the lower the thermal energy utilization value.

C. GENERALIZED TRANSFER EQUATION OF EXERGY

1) EXTENSIVE QUANTITY TRANSFER MODEL

The strength difference is a generalized force, which can promote the flow of the extensive quantity. Therefore, the calculation formula of the extensive amount of unit time flowing through unit area is as follows:

$$J_i = -k_i \nabla \chi_i, \tag{4}$$

where k_i is the transmission coefficient of the extensive quantity. We can easily obtain the formula of extensional flow:

$$\varphi_i = J_i A. \tag{5}$$

Combining (4) and (5), we can deduce the resistance of the extensive extension of the steady-state process, which is expressed by the resistance element. The resistive element R_i is equal to the generalized force divided by the extensor.

$$\begin{aligned} \varphi_i &= -k_i \nabla \chi_i A \\ \Rightarrow R_i &= \int_0^L \frac{1}{k_i A} dl = \frac{L}{k_i A}. \end{aligned} \tag{6}$$

The exergy flux density is obtained by multiplying the left and right sides of equation 4 $(\chi_i - \chi_{i0})$. In addition, after introducing the energy level factor, the expression of exergy flux density is as follows.

$$J_{Exi} = -(\chi_i - \chi_{i0}) k_i \nabla \chi_i = -\chi_i k_i \varepsilon_i \nabla \chi_i = -\lambda_i \varepsilon_i \nabla \chi_i, \tag{7}$$

where $\lambda_i = \chi_i k_i$ is the energy transfer coefficient.

2) EXERGY TRANSFER EQUATION IN A LINE

Combining the continuity axiom and Lagrange method, the dynamic equilibrium equation of exergy transfer is obtained as follows.

$$\rho_i \frac{dE_{xi}}{dt} = -\nabla \cdot \mathbf{J}_{Exi} + \mathbf{J}_i \cdot \nabla \chi_i + (\chi_i - \chi_{i0}) \sigma_i, \tag{8}$$

where the left side of the equals sign is the change of exergy with time in unit volume. On the right side of the equals sign, the first item is the exergy of the net inflow volume element boundary, the second item is the exergy generated by the mutual conversion of different forms of exergy promoted by the intensity difference, and the third item is the exergy generated with the basic extensive quantity source.

D. ENERGY NETWORK EQUATION

Considering the extensive flow and intensive quantity of each branch in the energy network as variables, these variables are subject to two kinds of constraints: topological constraints and component constraints. According to these two kinds of constraints, the values of variables can be calculated.

1) TOPOLOGICAL CONSTRAINTS

The generalized Kirchhoff's law, including Kirchhoff's law of extension (KEL) and Kirchhoff's law of intensity (KIL), is established in the energy network by analogy based on circuit science. KEL means that in a centralized energy network, the algebraic sum of the branch extensive flow of all outgoing nodes is equal to zero for any node at any time. KIL means that in a concentrated energy network, the algebraic sum of all branch intensive quantities is equal to zero at any time along any loop.

KEL and KIL add topological linear constraints to the energy network. These constraints are only related to the connections between components, not to the properties of components, that is, whether or not the components are linear or time invariant, the constraints are always tenable.

2) COMPONENT CONSTRAINTS

According to the characteristics of the elements in the energy network, the relationship between the extensive flow and the intensive quantity can be formed. For example, the relationship between the extensive flow and the intensive quantity of the linear resistive elements must satisfy $\chi_i = R_i \cdot \varphi_i$.

According to the topological and component constraints, the energy network equation can be established, and the network state variables can be solved.

III. CHARACTERISTIC TRANSMISSION LAW OF EXERGY IN A LINE

In an IES, the energy transfer lines are usually cylindrical. Therefore, by integrating the left and right sides of (8) at the same time, the transfer equation of exergy from section m to section n of the cylindrical energy transfer line is obtained as follows. For brevity, the subscript i is omitted.

$$\frac{\mathrm{d}E_x}{\mathrm{d}t} = (\chi_\mathrm{m} - \chi_0)\,\varphi_\mathrm{m} - (\chi_\mathrm{n} - \chi_0)\,\varphi_\mathrm{n} + \int_\mathrm{m}^\mathrm{n} \varphi \mathrm{d}\chi + \int_\mathrm{m}^\mathrm{n} (\chi - \chi_0)\,\mathrm{d}x_g. \quad (9)$$

For the time invariant system, the left and right sides of the equation are equal to zero. The first and second terms on the right side of the equation are the exergy loss of the energy flow process in a line, as shown in (10).

$$\begin{aligned}\Delta P_x &= (\chi_\mathrm{m} - \chi_0)\,\varphi_\mathrm{m} - (\chi_\mathrm{n} - \chi_0)\,\varphi_\mathrm{n} \\ &= -\int_\mathrm{m}^\mathrm{n} \varphi \mathrm{d}\chi - \int_\mathrm{m}^\mathrm{n} (\chi - \chi_0)\,\mathrm{d}x_g. \end{aligned} \quad (10)$$

From (10), it can be deduced that the loss consists of two parts, i.e., the energy loss ΔE in the transfer process and the energy loss caused by irreversibility $\chi_0 \Delta\varphi$.

$$\Delta P_x = \chi_\mathrm{m}\varphi_\mathrm{m} - \chi_\mathrm{n}\varphi_\mathrm{n} + \chi_0\,(\varphi_\mathrm{n} - \varphi_\mathrm{m}) = \Delta P + \chi_0 \Delta\varphi. \quad (11)$$

Since the power at the entrance section m of the line is $P_{xm} = AJ_{Ex}$, combining with (7), the variation rule of the intensive quantity along the line can be deduced as follows.

$$\begin{aligned} P_m &= AJ_E = -A\lambda\nabla\chi \\ \Rightarrow \chi_n &= \chi_m - \frac{L}{A\lambda}P_m = \chi_m - \frac{R}{\chi_m}P_m. \end{aligned} \quad (12)$$

Combining (11) and (12), the exergy power loss equations of different energy transfer processes and the intensity distribution equations along the energy transfer line in a time invariant energy network are derived as follows.

A. ELECTRICAL ENERGY NETWORK

In a power network, electrical exergy represents the ability of the electrified system to make the most useful work to the relevant object under the action of an electric field. Generally, the earth is taken as the zero potential point, the static state value of the potential χ_{e0} is equal to zero, and the electric energy level is equal to one, so the electrical exergy change is the same as the electrical energy change, as shown in the following formula.

$$\begin{cases} \Delta P_{x\mathrm{e}} = \Delta P_\mathrm{e} \\ \Rightarrow P_{x\mathrm{en}} = P_{x\mathrm{em}} - R_\mathrm{e}\left(\dfrac{P_{x\mathrm{em}}}{\chi_\mathrm{em}}\right)^2, \end{cases} \quad (13)$$

where $R_\mathrm{e} = \frac{L}{k_\mathrm{e}A}$, in which k_e represents conductivity.

Cylindrical metal wire is often used for common cables and overhead lines in the project, and the current is essentially formed by the electronic flow. Therefore, under the condition of time invariant (DC), the distribution of the basic intensive quantity (voltage) along the line in the process of power transmission also satisfies (12). Then:

$$\chi_{en} = \chi_{em} - R_e\frac{P_{em}}{\chi_{em}}, \quad (14)$$

where the subscript e indicates that the basic quantity corresponds to the electric energy transmission state.

B. HEAT ENERGY NETWORK

In this section, the incompressible fluid is used as the heat transfer medium to analyze the heat transfer law in the line. The specific heat capacity can be regarded as a fixed value in the case of little temperature change. The calculation formula of entropy increase for the heat transfer line of incompressible fluid is as follows.

$$\Delta\varphi_\mathrm{h} = c\rho\varphi_\mathrm{p} \ln\frac{\chi_\mathrm{hm}}{\chi_\mathrm{hn}}. \quad (15)$$

In the process of heat transfer between pipe section m and n, the calculation formula of heat energy change is as follows.

$$\Delta P_\mathrm{h} = c\rho\varphi_\mathrm{p}\,(\chi_\mathrm{hm} - \chi_\mathrm{hn})\,. \quad (16)$$

Combining (11), (15) and (16), the calculation formula of heat exergy loss in the line is obtained as follows.

$$\begin{aligned}\Delta P_{\mathrm{xh}} &= \Delta P_{\mathrm{h}} + \chi_{h0}\Delta\varphi_{\mathrm{h}} \\ &= c\rho\varphi_{\mathrm{p}}\left(\chi_{\mathrm{hm}} - \chi_{\mathrm{hn}} + \chi_{h0}\ln\frac{\chi_{\mathrm{hm}}}{\chi_{\mathrm{hn}}}\right),\end{aligned} \tag{17}$$

where χ_{h0} is the temperature silent value, which is generally considered equal to the ambient temperature.

The temperature at the end of the heat transfer line χ_{hn} in (17) can be obtained by the temperature drop formula of the heat transfer line, as shown in the following formula.

$$\chi_{hn} = \chi_{h0} + (\chi_{hm} - \chi_{h0})\exp\left(-\frac{\lambda_{\mathrm{h}}L}{c\rho\varphi_{\mathrm{p}}}\right), \tag{18}$$

where λ_{h} is the heat transfer coefficient of the insulated heat transfer line.

C. PRESSURE ENERGY NETWORK

In this section, the steady-state laminar flow of incompressible fluid is used to analyze the loss of pressure exergy in the line. Although the static value of pressure is not equal to zero, because the volume source of incompressible fluid is equal to zero, the change of pressure exergy is equal to the change of pressure energy. The expression of pressure exergy loss is as follows.

$$\Delta P_{\mathrm{xp}} = \Delta P_{\mathrm{p}} = \varphi_{\mathrm{p}}^2 R_{\mathrm{p}}, \tag{19}$$

where R_{p} is the fluid flow resistance which is calculated as $R_{\mathrm{p}} = \frac{L}{k_{\mathrm{p}}A} = \frac{8\rho\varphi_{\mathrm{v}}Lf}{D^5\pi^2}\left(kg/(m^4\cdot s)\right)$.

IV. OPERATION OPTIMIZATION MODEL OF IES CONSIDERING EXERGY

In this section, the IES operation optimization model considering the exergy loss of different types of energy during the transmission process is established to obtain the optimal operational strategy with higher efficiency and quality of energy utilization.

A. OBJECTIVE FUNCTION

In detail, the objective function includes the exergy loss costs of electricity, heat, and pressure in the IES. Note that the cost for different types of exergy loss is different, which is also considered in this paper and expressed as follows.

$$\begin{aligned}\min C_{loss} = c_{\mathrm{xe}}\Big(\sum_{i\in S_{\mathrm{el}}}\Delta P_{xe}^{i} + \sum_{i\in S_{\mathrm{hl}}}\Delta P_{xp}^{i}\Big/\eta_{\mathrm{p}}\Big) \\ + c_{\mathrm{xh}}\sum_{i\in S_{\mathrm{el}}}\Delta P_{x\mathrm{h}}^{i}.\end{aligned} \tag{20}$$

Note that, since the pressure exergy loss ΔP_{xp}^{i} can be directly reflected by the electrical exergy loss ΔP_{xe}^{i}, the cost corresponding to the pressure exergy loss can be expressed by that of the electrical exergy loss after the pressure power is converted into electrical power. Here, η_{p} denotes the conversion coefficient of pressure power and electrical power, which is equal to the efficiency coefficient of the circulating water pump.

It is worth pointing out that the values of c_{xe} and c_{xh} can greatly influence the obtained solution. To avoid over subjectively determining their values, a relatively objective approach based on energy level factor ε and the cost of producing energy is proposed, which is expressed as follows.

$$\begin{cases}P_{\mathrm{xe}} = (1-\frac{\chi_{e0}}{\chi_e})P_{\mathrm{e}} \\ c_{\mathrm{e}}P_{\mathrm{e}} = c_{\mathrm{xe}}P_{\mathrm{xe}}\end{cases} \xrightarrow{\varepsilon_{\mathrm{e}}=(1-\frac{\chi_{e0}}{\chi_e})} c_{\mathrm{xe}} = \frac{1}{\varepsilon_{\mathrm{e}}}c_{\mathrm{e}}, \tag{21}$$

$$\begin{cases}P_{\mathrm{xh}} = (1-\frac{\chi_{h0}}{\chi_h})P_{\mathrm{h}} \\ c_{\mathrm{h}}P_{\mathrm{h}} = c_{\mathrm{xh}}P_{\mathrm{xh}}\end{cases} \xrightarrow{\varepsilon_{\mathrm{h}}=(1-\frac{\chi_{h0}}{\chi_h})} c_{\mathrm{xh}} = \frac{1}{\varepsilon_{\mathrm{h}}}c_{\mathrm{h}}, \tag{22}$$

where c_{e} and c_{h} represent the costs of producing electrical energy and thermal energy, respectively. In particular, since the value of the electrical energy level factor ε_{e} is equal to one, we can obtain that $c_{\mathrm{xe}} = c_{\mathrm{e}}$.

B. ELECTRICAL RESTRAINT

The active power P_e^G and reactive power Q_e^G outputs of generators are limited within lower and upper bounds, expressed as follows.

$$P_{\mathrm{e}}^{G_{min}} \le P_e^G \le P_e^{G_{max}}. \tag{23}$$

$$Q_e^{\mathrm{G}_{min}} \le Q_e^G \le Q_e^{\mathrm{G}_{max}}. \tag{24}$$

The magnitude χ_{e} and phase angle θ_{e} of load nodes are also limited within a reasonable range to ensure the safe operation of the electrical energy network.

$$\chi_{emin} \le \chi_{\mathrm{e}} \le \chi_{\mathrm{e\,max}}. \tag{25}$$

$$\theta_{\mathrm{e\,min}} \le \theta_{\mathrm{e}} \le \theta_{\mathrm{e\,max}}. \tag{26}$$

The apparent power flow on each energy transmission line should be no more than its capacity value.

$$P_{\mathrm{e}}^{l2} + Q_{\mathrm{e}}^{l2} \underset{l\in s_{\mathrm{el}}}{\le} \chi_{\mathrm{e}}^2\varphi_{\mathrm{emax}}^{l2}. \tag{27}$$

For the electrical energy network with transformers, the transformer ratios Tap_i, which are important decision-making variables, should be subject to the following the upper and lower limits of regulation of transformer tap:

$$Tap_{i\,\min} \le Tap_i \le Tap_{i\,\max},\ i \in S_{Tap}. \tag{28}$$

Finally, the power balance constraints related to the active power and reactive power in each node should be satisfied to ensure the stability of frequency and voltage.

$$\underset{k\in N_e}{P_{\mathrm{e},k}} = \chi_{U,k}\sum_{g\in k}\chi_{U,g}\left(G_{kg}\cos\theta_{kg} + B_{kg}\sin\theta_{kg}\right), \tag{29}$$

$$\underset{k\in N_e}{Q_{\mathrm{e},k}} = \chi_{U,k}\sum_{g\in k}\chi_{U,g}\left(G_{kg}\sin\theta_{kg} - B_{kg}\cos\theta_{kg}\right), \tag{30}$$

where N_{e} is the quantity of nodes in the power network; k represents the node number of the power network, and $g \in k$ means node g is the associated node of node k; $P_{\mathrm{e},k}$ and $Q_{\mathrm{e},k}$ are the net injected active power and the net injected reactive power of node k, respectively; and G_{kg}, B_{kg} and θ_{kg} are the conductance, susceptance, and phase angle difference between nodes k and g, respectively.

C. HYDRAULIC-THERMAL RESTRAINT

Note that the thermal outputs of gas-fired boilers $P_{\mathrm{h}}^{\mathrm{G}}$ are limited by lower and upper bounds. Thus, the outputs of each node in a heat energy network should be kept within a limited range.

$$P_{\mathrm{h}}^{\mathrm{G}\min} \leq P_{\mathrm{h}}^{\mathrm{G}} \leq P_{\mathrm{h}}^{\mathrm{G}\max}. \tag{31}$$

Similarly, the water temperature of each node in a heat energy network should be enforced within a limited range due to their limited ranges.

$$\chi_{\mathrm{h}\,\min} \leq \chi_{\mathrm{h}} \leq \chi_{\mathrm{h}\,\max}. \tag{32}$$

Note that the service life of thermal lines is associated with the heat power p_{h}^{l} transmitted through the lines. Thus, the heat power should also meet the constraints of its minimum and maximum power limits.

$$P_{\mathrm{h}}^{l\min} \leq P_{\mathrm{h}}^{l} \leq P_{\mathrm{h}}^{l\max}. \tag{33}$$

In addition, the space of the lines is limited, and thus water flow within the lines should not exceed the largest values.

$$\varphi_{\mathrm{p}\,\min} \leq \varphi_{\mathrm{p}} \leq \varphi_{\mathrm{p}\,\max}. \tag{34}$$

Similar to the electrical energy network, the heat power balance constraint in each node is required to satisfy the heat demands.

$$\sum_{a\in N_{\mathrm{h}}} P_{\mathrm{h},a} - \sum_{b\in N_{\mathrm{h}}} P_{\mathrm{h},b} = \sum_{d\in N_{\mathrm{hl}}} \Delta P_{h,d}, \tag{35}$$

where N_{h} is the number of nodes in the power network; N_{hl} is the total number of thermal lines in the heat network; d is the line number of the thermal network; a and b are the associated input node number and associated output node number of line d, respectively; $P_{\mathrm{h},a}$ is the net inflow thermal power of node a and $P_{\mathrm{h},b}$ is the net outflow thermal power of node b; and $\Delta P_{h,d}$ is the heat loss of pipe d.

There are also heat balance constraints at the mixing nodes.

$$\rho \sum_{d_j\in S_d} \varphi_{\mathrm{p},a}^{d_j} \chi'_{\mathrm{h},a} = \sum_{a_j\in S_a, d_j\in S_d} \rho \varphi_{\mathrm{p},a}^{d_j} \chi'_{\mathrm{h},a_j}, \tag{36}$$

where b_j is the inflow pipe associated with node a; S_d is the collection of all pipes associated with the node a_j; a_j is the inlet node of the inflow pipe associated with node a; S_d is the set of hybrid nodes a_j; and $\chi'_{\mathrm{h},a}$ is the difference between the temperature of node $a\,\chi_{\mathrm{h},a}$ and the ambient temperature $\chi_{\mathrm{h}0}$.

D. ENERGY-COUPLING EQUIPMENT

1) CHP UNITS

According to whether the thermal power ratio of the combined heat and power (CHP) unit changes, it can be divided into two types: constant thermal power ratio Z_{const} (such as gas turbines and reciprocating internal combustion engines) and variable thermal power ratio $Z_{vriable}$ (such as extraction turbines). The relationships between the heat and electricity produced are shown in (38) and (39).

$$Z_{const} = \frac{P_{\mathrm{h}}^{G}}{P_{\mathrm{e}}^{G}}, \tag{37}$$

$$Z_{vriable} = \frac{P_{\mathrm{h}}^{G}}{\eta_{\mathrm{e}} F_{in} - P_{\mathrm{e}}^{G}}, \tag{38}$$

where η_{e} is the condensation efficiency of the CHP unit and F_{in} is the fuel input rate.

2) WATER CIRCULATING PUMP

The circulating water pump converts the electrical energy into the pressure energy, which is used to overcome the resistance encountered in the transmission process of the thermal quality in the thermal network. The calculation expression of the electrical power consumed by the circulating water pump P_{pump} is as follows:

$$P_{\mathrm{pump}} = \frac{\varphi_{\mathrm{p}} g \chi_{\mathrm{p}}}{10^6 \eta_{\mathrm{p}}}, \tag{39}$$

where φ_{p} is the mass flow rate of the hot working medium in the pump; g is the acceleration of gravity; χ_{p} is the pump pressure at the outlet of the circulating water pump; and η_{p} is the pump efficiency coefficient.

E. GENETIC ALGORITHM BASED ON ADAPTIVE ELITIST RETENTION STRATEGY

Note that the proposed model is a complex, non-convex, non-linear optimization problem that can be expressed as the following general form.

$$\min\ f(\boldsymbol{X}) \tag{40}$$

$$s.t.\ \begin{cases} g_v(\boldsymbol{X}) \geq 0, & v = 1, 2, \cdots V \\ h_o(\boldsymbol{X}) = 0, & o = 1, 2, \cdots O \end{cases} \tag{41}$$

where $\boldsymbol{X}$ denotes the decision-making variables, including θ_{e}, χ_{e}, φ_{p}, χ_{h}, ΔP_{xe}, ΔP_{xh}, and ΔP_{xp}; the expressions of $f(\cdot)$, $g_v(\cdot)$, and $h_o(\cdot)$ represent the objective function, inequality constraints, and equality constraints, respectively. Conventional algorithms cannot solve this model. Here, an artificial algorithm, i.e., an adaptive GA, is developed to solve the proposed model. GA does not have strong requirements for the convexity, continuity, or differentiability of the model to be solved, and it can seek the global optimal solution with random methods. GA regards the solution set of the problem as a population and improves the quality of the solution through continuous selection, crossover, variation, and other genetic operations. The detailed convergence performance of the GA is proved in the work of He and Kang [28]. The solving process is provided as follows.

Step 1: Set the input data of energy networks and parameters of the GA. The input data mainly include the load demands of electrical power and thermal power, and the parameters of transmission lines in electrical, heat, and pressure energy networks. The parameters consist of the population *Pop*, probability of mutation p_m, probability of crossing p_c and maximum of the genetic iteration $\mathrm{T}_{\max}$.

Step 2: Initialize the population of the GA. The population consists of a series of individuals (i.e., decision-making variables $\boldsymbol{X}$), represented as $(\boldsymbol{X}^1, \boldsymbol{X}^2, \ldots, \boldsymbol{X}^{Pop})$. Note that all generated individuals should be located in feasible regions of the model.

Step 3: Perform crossover operation based on probability of crossing p_c. First, the individuals in the population are extracted at the probability p_c and randomly divided into pairs. Then, for each pair $(\boldsymbol{X}^i, \boldsymbol{X}^j)$, we perform the following operation:

$$\boldsymbol{X}^{i*} = c\boldsymbol{X}^i + (1-c)\boldsymbol{X}^j, \tag{42}$$

$$\boldsymbol{X}^{j*} = c\boldsymbol{X}^j + (1-c)\boldsymbol{X}^i, \tag{43}$$

where c is a randomly generated parameter located in (0, 1). Note that if the newly generated individuals $\boldsymbol{X}^{i*}$ and $\boldsymbol{X}^{j*}$ are not located in feasible regions of the model, a new value of c should be randomly generated, and the above process (43)–(44) should be repeated until the obtained $\boldsymbol{X}^{i*}$ and $\boldsymbol{X}^{j*}$ are located in feasible regions.

Step 4: Commit mutation operation according to probability of mutation p_m. First, we sample the population that finishes the crossover operation with probability p_m. Then, for each sampled individual $\boldsymbol{X}^i$, the following operation is committed:

$$\boldsymbol{X}^{i0} = \boldsymbol{X}^i + D\boldsymbol{d}, \tag{44}$$

where $\boldsymbol{d}$ represents the direction of mutation, and its value is restricted within $(-1, 1)$; D denotes the amplification. Similar to Step 3, the newly obtained individuals $\boldsymbol{X}^{i0}$ should be located in feasible regions. Otherwise, new values of $\boldsymbol{d}$ and D should be changed randomly until $\boldsymbol{X}^{i0}$ are located in feasible regions.

Step 5: Sort the individuals in the obtained population. Note that, since the proposed model minimizes the objective function, the fitness function y is set by

$$y = 1/C_{loss}. \tag{45}$$

After the calculation, the individuals in the newly obtained population are reordered in ascending order based on the values of the corresponding fitness function y.

Step 6: Select the individuals in the current population. In this step, the evaluation function is first calculated.

$$\begin{cases} q(i) = q(i-1) + y^i, 1 \le i \le Pop \\ q(0) = 0 \end{cases} \tag{46}$$

Then, the current population is filtered by adopting the Roulette method. In detail, we first generate a random parameter r_q within (0, 1), and if $r_q q(Pop) \in [q(i-1), q(i)]$, then the ith individual $\boldsymbol{X}^i$ is selected as a member of the next population. By repeating this operation Pop times, a new population can be obtained.

Step 7: Judge whether the current loop iteration T is larger than the threshold $T_{\max}$. If not, go back to Step 2 and perform Steps 2–6. Otherwise, output the optimal solution $\boldsymbol{X}^*$ as well as the corresponding objective function C^*_{loss}. The flowchart is provided in Fig. 2.

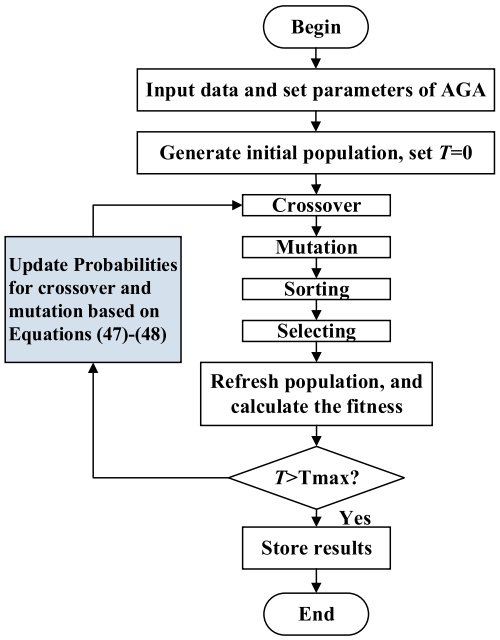

FIGURE 2. Genetic algorithm flowchart with elite retention strategy.

It is worth pointing out that, compared with standard GA, two improvements of the GA are proposed to accelerate the speed of finding the optimal solution, stated as follows.

Improvement 1: In the standard GA, the selected process mostly uses the Roulette method, which selects individuals with higher fitness values y by generating random values. However, due to statistical errors, individuals with higher fitness values y may also be excluded, leading to suboptimal results. Here, an elite retention strategy is employed to prevent individuals with high fitness values y in the current population from being eliminated in the next population. In detail, the individuals with high fitness that appear in the evolution process are collected and directly copied to the next generation of population without crossing and mutating steps. The new generation of populations treated with the elite retention strategy are reordered, and the corresponding number of individuals with the lowest fitness are eliminated to ensure the number of populations. Although the increase in the number of population elites can accelerate the convergence of the algorithm, too large of an increase will reduce the diversity of the individuals, resulting in the algorithm prematurely falling into local solutions. Therefore, in this paper, only the best individuals of the population are reserved as elites to ensure that the solution is approximately optimal.

Improvement 2: The standard GA usually assumes that the crossover probability and mutation probability are constants pre-set before the optimization. In this paper, a flexible GA is adopted to improve the global searching performance and convergence speed of the algorithm. The detailed formulation of the flexible approach can be expressed as

TABLE 1. The detailed settings of the algorithms.

Parameters	Generations T	Populations Pop	Crossover Probability	Mutation Probability
			p_c	p_m
Values	50	50	0.9	0.01

follows.

$$p_c = \begin{cases} p_{cmax} - \dfrac{(p_{cmax} - p_{cmin})(y' - y_{avg})}{y_{max} - y_{avg}} & y' \geq y_{avg} \\ p_{cmax} & y' < y_{avg}, \end{cases} \tag{47}$$

$$p_m = \begin{cases} p_{mmax} - \dfrac{(p_{mmax} - p_{mmin})(y - y_{avg})}{y_{max} - y_{avg}} & y \geq y_{avg} \\ p_{mmax} & y < y_{avg}, \end{cases} \tag{48}$$

where y_{max} and y_{avg} denote the maximum and average fitness of the population in the GA, respectively; y' is the larger fitness of the two individuals to be crossed; y is the fitness of the mutated individuals; $p_{c\,max}$ and $p_{c\,min}$ are the maximum and minimum values of the crossover probability, respectively; and p_{mmax} and p_{mmin} are the maximum and minimum values of the mutation probability, respectively. Thus, through the adaptive adjustment formula of crossover probability and mutation probability, for the individuals with below-average fitness, the higher crossover probability and mutation probability are used to eliminate the solution with a higher probability, whereas for the individuals with above-average fitness, the lower crossover probability and mutation probability are employed to retain the solution with a higher probability in the next generation. The detailed settings of the algorithms are provided in Table 1.

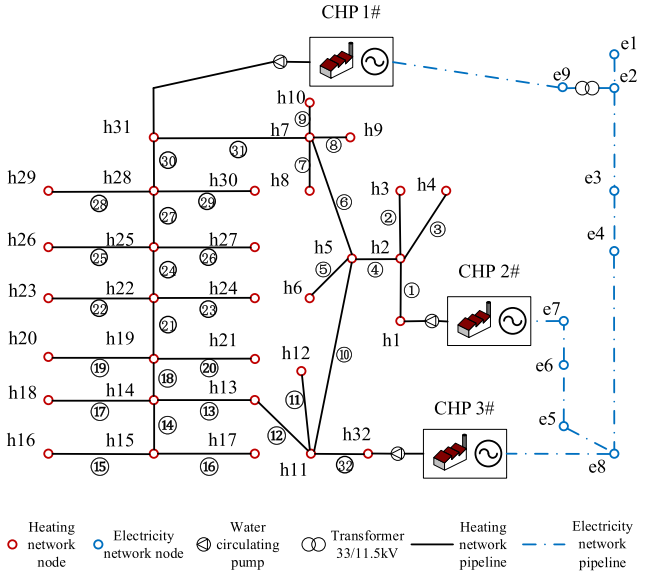

FIGURE 3. The topology of the Bali electricity-heat interconnection IES.

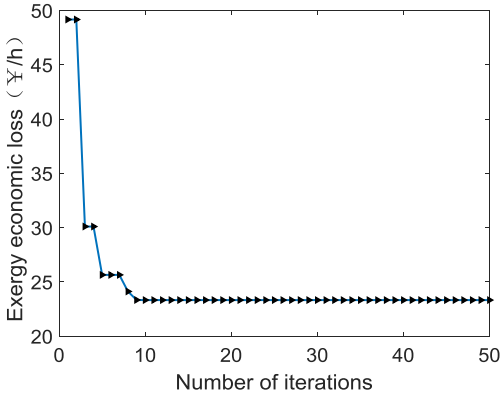

FIGURE 4. Convergence curve of exergy economic loss.

V. CASE STUDY

In order to study the operation optimization of IESs considering the economic exergy loss, we conduct a case study. We select the Bali electricity-heat interconnection IES as the subject of the study, and its topology is shown in Fig. 3. The system consists of a 33-node thermal network and a 9-node power network. The water supply and return pipes of the thermal network are symmetrical. The power network is equipped with a transformer and operates in an isolated network. The system is supplied with energy by three cogeneration units with a lithium bromide absorption chiller. The No.1 and No.3 CHP units are gas turbines, and the No.2 CHP unit is a set of extraction steam turbines. Three circulating water pumps are connected at the outlet of the CHP units to drive the flow of working water. The thermal load of the thermal network and the electrical load of the power network are known based on the information provided in [29].

It is assumed that node e9 is the slack node of the power grid, node h1 is the slack node of the heat grid and the ambient temperature is 10°C. The control variables are the outlet temperature of three heating nodes, the voltage amplitude of three power nodes, and the transformer ratio. The state variables include the voltage amplitude and phase angle of the grid line nodes and the mass flow and temperature of each node in the heat supply network.

A. ITERATIVE CONVERGENCE CURVE

We mark the exergy economic loss value corresponding to the optimal individual selected in each iteration with a triangle symbol and then connect the triangles to draw the convergence curve as shown in Fig. 4. It can be seen from the figure that the exergy economic loss curve of this example basically reaches convergence after 10 iterations, with good convergence ability and fast convergence speed.

B. STATE VARIABLE ANALYSIS

The optimal value of the objective function and control variable can be obtained by the improved GA. By decoding the optimal gene individuals, the changes of voltage amplitude

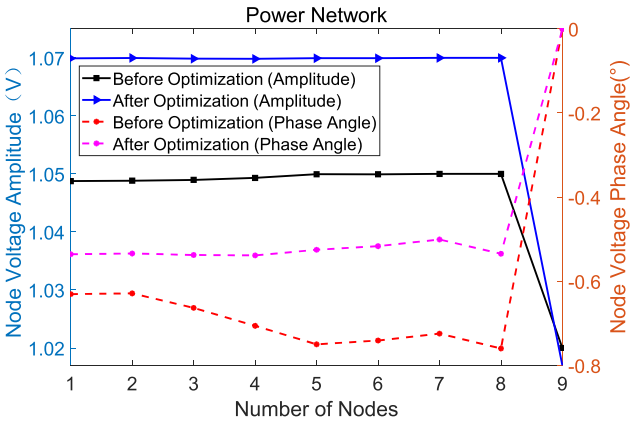

FIGURE 5. Comparison of voltage amplitude and phase angle before and after optimization.

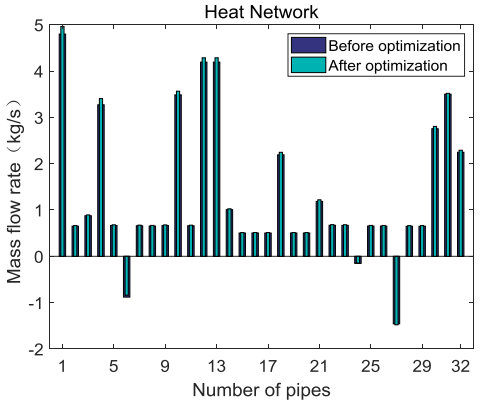

FIGURE 6. Comparison of mass flow rate of nodes before and after optimization.

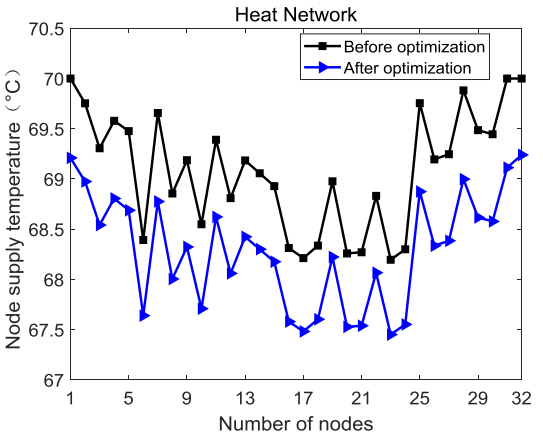

FIGURE 7. Node supply temperature before and after optimization.

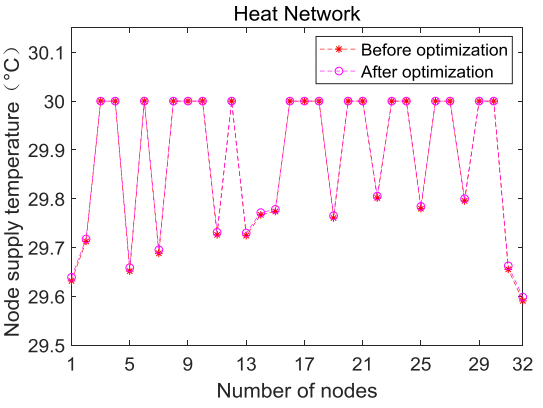

FIGURE 8. Node return temperature before and after optimization.

and phase angle, line mass flow, node supply temperature, and node return temperature of each node before and after optimization are shown in Fig. 5, Fig. 6, Fig. 7, and Fig. 8, respectively.

It can be seen from Fig. 5 that the voltage amplitude of nodes increases after optimization, but the amplitude of each node only changes slightly, with the maximum value being only approximately 0.02 V. The optimized node voltage phase angle is closer to the zero phase, which causes the line loss to be reduced. The optimized results are obviously more conducive to reducing the power loss of the system with a high exergy price.

In Fig. 6, the mass flow of the line is drawn in the form of a histogram, and the positive and negative values in the figure represent the flow direction of the mass flow of the line. It can be seen that after optimization, the mass flow in the line basically remains the same; only part of the line mass flow has a small increase. As the control variable in the heat supply network of this example is the outlet temperature of the CHP unit, it is necessary to further analyze the temperature of each heat node.

In Fig. 7, the node supply temperatures before and after optimization are represented by a black line chart and a blue line chart, respectively. After optimization, the supply temperatures of all heating nodes are reduced to varying degrees. The decrease of node temperature indicates the weakening of heating capacity. In Fig. 8, the return temperature of each node is basically unchanged, which is because the outlet temperature of the thermal load in this calculation example remains unchanged, so only a small number of intermediate nodes and heat source nodes will have a small change in the return temperature.

According to the analysis of the comparison diagram before and after the optimization of the state variables of the IES, when the thermal network supplies heat energy, the node temperatures change greatly, whereas the mass flow in the line changes little. This is because the difference between the unit supply temperature and the ambient temperature is large, so it is more economical and reasonable to optimize the thermal exergy of the system. Therefore, when the supply temperature of the unit is not much different from the ambient temperature, such as in summer, quantities regulation can be used to optimize the pressure exergy of the system.

C. EXERGY ECONOMIC ANALYSIS

After adopting the IES optimization model, the system optimization results are shown in Fig. 9(a) under the condition

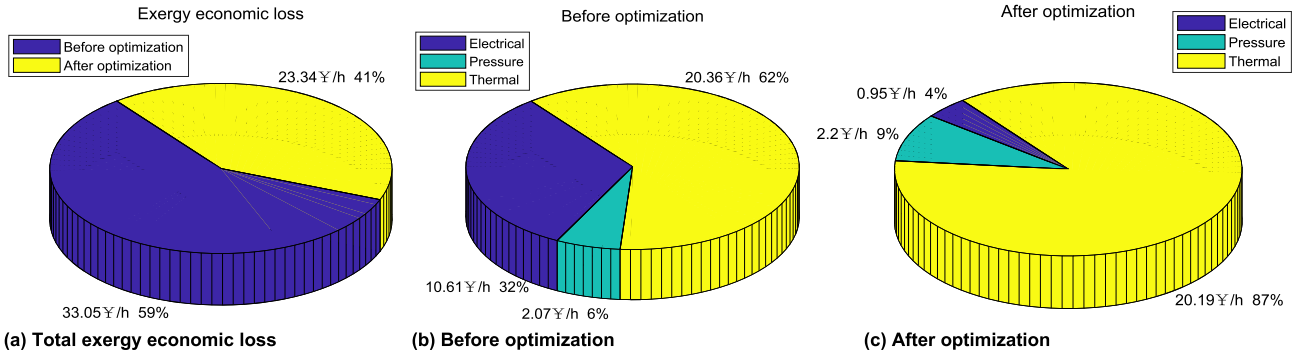

FIGURE 9. Comparison of exergy economic loss in Bali Island before and after optimization.

that the system parameters have little change. The exergy economic loss of the original island IES is 33.05 ¥/h, which is 23.34 ¥/h after optimization. The total exergy economic loss of the system is reduced by 29.4%, which effectively improves the energy utilization efficiency of the IES and proves the effectiveness of the proposed method.

Fig. 9(b) shows the proportion of exergy economic loss before optimization, and Fig. 9(c) shows the proportion of exergy economic loss after optimization. It can be seen from Fig. 9(b) and Fig. 9(c) that the proportion of economic loss of electrical exergy decreases from 32% to 4%, the proportion of economic loss of pressure exergy increases slightly from 6% to 9%, and the proportion of economic loss of thermal exergy increases from 62% to 87%. It is worth noting that the economic loss of thermal exergy basically remains unchanged before and after optimization. From this analysis, it can be seen that the IES optimization based on the exergy economic standard mainly focuses on the optimization of electrical energy, which is caused by the higher unit price of electrical energy, because the work ability of electrical energy power is much stronger than the lower grade thermal energy.

D. EFFECT OF AMBIENT TEMPERATURE ON EXERGY ECONOMIC ANALYSIS

It is assumed that the price of heat energy is constant at different ambient temperatures. Since the ambient temperature will affect the energy level of thermal energy, the corresponding heat exergy price is different according to formula 22. Combined with formula 20, it can be seen that the objective function also changes with the ambient temperature. Therefore, we give a temperature sensitivity analysis of thermal exergy loss, pressure exergy loss, and electrical exergy loss in the energy network, as shown in Fig. 10.

As the temperature changes from 0°C to 20°C (in steps of 5°C), the total exergy loss in the energy network is gradually decreasing, of which the thermal exergy loss accounts for the bulk. When the ambient temperature increases, the heating demand of the unit is weakened, and the heat energy loss in the network is also significantly reduced. Although the work capacity of heat energy is also weakened, the irreversible loss of heat energy wasted to the environment increases with the increase of ambient temperature, but this

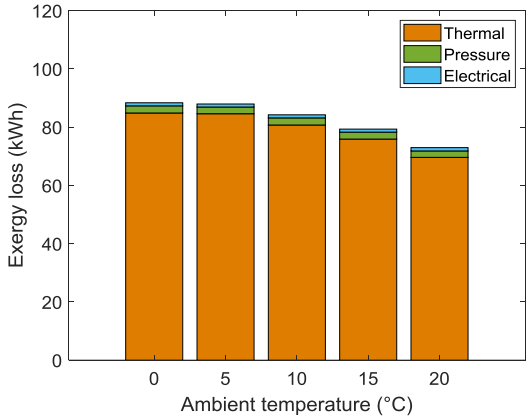

FIGURE 10. Effect of ambient temperature on thermal/ pressure/ electrical exergy loss.

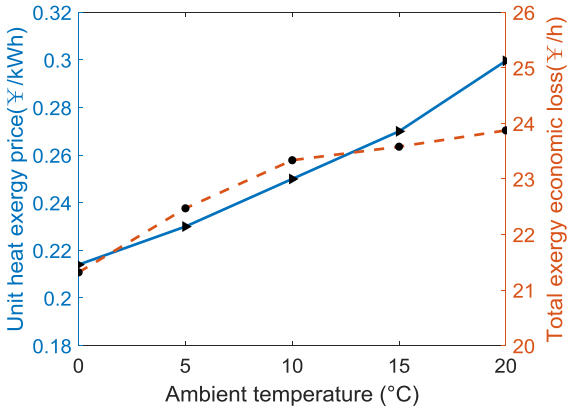

FIGURE 11. Effect of ambient temperature on unit heat exergy price and total exergy economic loss.

part of the loss is relatively small. Therefore, according to formula 17, the total exergy loss in the network is gradually reduced.

According to formula 22, the heating exergy price at different ambient temperatures can be obtained, as shown in the blue line with blue triangle marks in Fig. 11. When the price of thermal energy is constant, the energy level factor of thermal energy decreases with the increase of ambient temperature, while the price of thermal exergy is to the contrary. In the case of decreasing heat exergy loss and

increasing heating exergy price, the change of total exergy economic loss with ambient temperature is simulated as shown in the orange dashed-dotted line in Fig. 11. Because the thermal exergy loss decreases less with increasing ambient temperature, the increase of thermal exergy price is larger, and the electrical and pressure exergy losses account for a small proportion. Therefore, according to formula 20, the total exergy economic loss increases with increasing ambient temperature. The conclusion of this section is based on the analysis that the price of heat energy remains unchanged and will change under different ambient temperatures. The lower the ambient temperature, the greater the output of heating unit and the more exergy is lost by the network, but the lower the heating price. However, when applied to specific production and life scenarios, different assumptions must be made for reanalysis.

VI. CONCLUSION

This paper proposes a novel unified modeling theory to analyze the degradation of the energy transfer process in IESs, which lays a theoretical foundation for maximizing the energy efficiency of IESs. First, a method based on energy network theory is proposed to develop a unified rule of exergy transfer in different energy subnetworks: starting from energy network theory, and based on the idea of energy axiomatization, the steady-state transfer process of exergy in a thermal network and a fluid network is described in the form of an equivalent circuit, and the unified modeling of power networks, heating networks, and fluid networks is completed. Then, the calculation method of branch losses of different attributes of a comprehensive energy system under given conditions is given: the transfer law of a specific form of exergy in a cylindrical energy transfer line is given, including electrical exergy, thermal exergy, and pressure exergy. Then, considering the different values of exergy at different times and locations, a single period operation model of IES is established. Finally, based on the adaptive GA, the optimization result with the minimum exergy economic loss of IES as the objective function is solved quickly. Simulation results show the effectiveness of the proposed model and optimization method.

The exergy analysis method proposed in this paper is concise and unified, and the convergence effect is good through the adaptive GA. This analysis and simulation method can be extended to larger and more complex IESs. Through the optimization results of exergy loss analysis, it will be more accurate to point out the key parts of the energy consumption process to improve the energy efficiency of the system and provide reasonable energy guidance. The intelligent algorithm used in this paper easily deals with a strong nonlinear system, but the randomness of the population will bring uncertainty to the solution, so we must solve the problem many times to obtain the optimal value. This can be solved by other mathematical algorithms. Future work will seek the comprehensive evaluation method of IES optimization performance based on the principle of exergy economics theory.

REFERENCES

[1] Z. Liang, H. Chen, X. Wang, S. Chen, and C. Zhang, "Risk-based uncertainty set optimization method for energy management of hybrid AC/DC microgrids with uncertain renewable generation," *IEEE Trans. Smart Grid*, vol. 11, no. 2, pp. 1526–1542, Mar. 2020.

[2] W. Gu, Z. Wu, R. Bo, W. Liu, G. Zhou, W. Chen, and Z. Wu, "Modeling, planning and optimal energy management of combined cooling, heating and power microgrid: A review," *Int. J. Electr. Power Energy Syst.*, vol. 54, pp. 26–37, Jan. 2014.

[3] G. Yan, D. Liu, J. Li, and G. Mu, "A cost accounting method of the Li-ion battery energy storage system for frequency regulation considering the effect of life degradation," *Protection Control Mod. Power Syst.*, vol. 3, no. 1, pp. 43–51, Dec. 2018.

[4] H. S. V. S. K. Nunna and S. Doolla, "Demand response in smart distribution system with multiple microgrids," *IEEE Trans. Smart Grid*, vol. 3, no. 4, pp. 1641–1649, Dec. 2012.

[5] H. Cho, A. D. Smith, and P. Mago, "Combined cooling, heating and power: A review of performance improvement and optimization," *Appl. Energy*, vol. 136, pp. 168–185, Dec. 2014.

[6] Y. Cao, Q. Li, Y. Tan, Y. Li, Y. Chen, X. Shao, and Y. Zou, "A comprehensive review of energy Internet: Basic concept, operation and planning methods, and research prospects," *J. Mod. Power Syst. Clean Energy*, vol. 6, no. 3, pp. 399–411, May 2018.

[7] J.-Y. Wu, J.-L. Wang, and S. Li, "Multi-objective optimal operation strategy study of micro-CCHP system," *Energy*, vol. 48, no. 1, pp. 472–483, Dec. 2012.

[8] W. Gu, Z. Wang, Z. Wu, Z. Luo, Y. Tang, and J. Wang, "An online optimal dispatch schedule for CCHP microgrids based on model predictive control," *IEEE Trans. Smart Grid*, vol. 8, no. 5, pp. 2332–2342, Sep. 2017.

[9] B. Tan and H. Chen, "Stochastic multi-objective optimized dispatch of combined cooling, heating, and power microgrids based on hybrid evolutionary optimization algorithm," *IEEE Access*, vol. 7, pp. 176218–176232, 2019.

[10] N. Nikmehr and S. Najafi-Ravadanegh, "Optimal operation of distributed generations in micro-grids under uncertainties in load and renewable power generation using heuristic algorithm," *IET Renew. Power Gener.*, vol. 9, no. 8, pp. 982–990, Nov. 2015.

[11] J. Wang, H. Zhong, Q. Xia, C. Kang, and E. Du, "Optimal joint-dispatch of energy and reserve for CCHP-based microgrids," *IET Gener., Transmiss. Distrib.*, vol. 11, no. 3, pp. 785–794, Feb. 2017.

[12] Q. Xu, L. Li, X. Chen, Y. Huang, K. Luan, and B. Yang, "Optimal economic dispatch of combined cooling, heating and power-type multi-microgrids considering interaction power among microgrids," *IET Smart Grid*, vol. 2, no. 3, pp. 391–398, Sep. 2019.

[13] M. F. Tahir, C. Haoyong, K. Mehmood, N. Ali, and J. A. Bhutto, "Integrated energy system modeling of China for 2020 by incorporating demand response, heat pump and thermal storage," *IEEE Access*, vol. 7, pp. 40095–40108, 2019.

[14] M. Jadidbonab, A. Dolatabadi, B. Mohammadi-Ivatloo, M. Abapour, and S. Asadi, "Risk-constrained energy management of PV integrated smart energy hub in the presence of demand response program and compressed air energy storage," *IET Renew. Power Gener.*, vol. 13, no. 6, pp. 998–1008, Apr. 2019.

[15] H. Ge, F. Liu, H. Chen, and C. Zhang, "Coordinated optimization of district electricity and heating system based on genetic algorithm," in *Proc. IEEE PES Asia–Pacific Power Energy Eng. Conf. (APPEEC)*, Xi'an, Oct. 2016, pp. 1543–1547.

[16] Q. Wang, J. Liu, Y. Hu, and X. Zhang, "Optimal operation strategy of multi-energy complementary distributed CCHP system and its application on commercial building," *IEEE Access*, vol. 7, pp. 127839–127849, 2019.

[17] C. Zhang, Y. Xu, Z. Y. Dong, and L. F. Yang, "Multitimescale coordinated adaptive robust operation for industrial multienergy microgrids with load allocation," *IEEE Trans. Ind. Informat.*, vol. 16, no. 5, pp. 3051–3063, May 2020.

[18] J. Yang, N. Zhang, Y. Cheng, C. Kang, and Q. Xia, "Modeling the operation mechanism of combined P2G and gas-fired plant with CO_2 recycling," *IEEE Trans. Smart Grid*, vol. 10, no. 1, pp. 1111–1121, Jan. 2019.

[19] C. Zhang, Y. Xu, Z. Li, and Z. Y. Dong, "Robustly coordinated operation of a multi-energy microgrid with flexible electric and thermal loads," *IEEE Trans. Smart Grid*, vol. 10, no. 3, pp. 2765–2775, May 2019.

[20] H. Chen, M. Qiu, H. Ge, and M. Li, "The application of energy network theory in the analysis of district electricity and heating system," in *Proc. IEEE Int. Conf. Energy Internet (ICEI)*, Beijing, China, Apr. 2017, pp. 36–41.

[21] P. Vivekh, D. T. Bui, M. R. Islam, K. Zaw, and K. J. Chua, "Experimental performance evaluation of desiccant coated heat exchangers from a combined first and second law of thermodynamics perspective," *Energy Convers. Manage.*, vol. 207, Mar. 2020, Art. no. 112518.
[22] R. Gaggioli, "Second law analysis for process and energy engineering," in *Proc. ACS Symp.*, vol. 235, 1983, pp. 3–50.
[23] M. Lozano and A. Valero, "Theory of the exergetic cost," *Energy*, vol. 18, no. 9, pp. 3–50, 1993.
[24] M. Ebrahimi, A. Keshavarz, and A. Jamali, "Energy and exergy analyses of a micro-steam CCHP cycle for a residential building," *Energy Buildings*, vol. 45, pp. 202–210, Feb. 2012.
[25] J. Wang, Z. Lu, M. Li, N. Lior, and W. Li, "Energy, exergy, exergoeconomic and environmental (4E) analysis of a distributed generation solar-assisted CCHP (combined cooling, heating and power) gas turbine system," *Energy*, vol. 175, pp. 1246–1258, May 2019.
[26] M. Abbasi, M. Chahartaghi, and S. M. Hashemian, "Energy, exergy, and economic evaluations of a CCHP system by using the internal combustion engines and gas turbine as prime movers," *Energy Convers. Manage.*, vol. 173, pp. 359–374, Oct. 2018.
[27] A. Mohammadi and M. Mehrpooya, "Energy and exergy analyses of a combined desalination and CCHP system driven by geothermal energy," *Appl. Thermal Eng.*, vol. 116, pp. 685–694, Apr. 2017.
[28] J. He and L. Kang, "On the convergence rates of genetic algorithms," *Theor. Comput. Sci.*, vol. 229, nos. 1–2, pp. 23–39, Nov. 1999.
[29] X. Liu, J. Wu, N. Jenkins, and A. Bagdanavicius, "Combined analysis of electricity and heat networks," *Appl. Energy*, vol. 162, pp. 1238–1250, Jan. 2016.

HAOYONG CHEN (Senior Member, IEEE) received the B.S., M.S., and Ph.D. degrees in electrical engineering from Xi'an Jiaotong University, Xi'an, China, in 1995, 1997, and 2000, respectively. He is currently a Professor with the School of Electric Power, South China University of Technology, Guangzhou, China. He is also the Chair of the Asia-Pacific Research Institute of Smart Grid and Renewable Energy, Kowloon, Hong Kong. His current research interests include power system operation/control, smart grids, computational intelligence applications, and power markets.

SIMIN CHEN (Student Member, IEEE) received the B.Eng. degree in electrical engineering and automation from Fuzhou University, Fuzhou, China, in 2018. She is currently pursuing the B.S. degree with the School of Electric Power Engineering, South China University of Technology, Guangzhou, China. Her research interests include modeling and operation optimization of the integrated energy systems.

MING LI received the bachelor's and master's degrees in electrical engineering from the South China University of Technology, Guangzhou, China, in 2017 and 2019, respectively. His research interest includes energy flow analysis of the integrated energy systems.

JINBIN CHEN received the B.Eng. degree in electrical engineering and automation from Fuzhou University, Fuzhou, China, in 2019. He is currently pursuing the master's degree in electrical engineering with the School of Electric Power, South China University of Technology, Guangzhou, China. His research interests include optimal operation of integrated energy systems and exergy analysis of multienergy flow systems.